Finite Element Analysis of Above-Ground Storage Tank Foundations on Soft Swamp Soils in Jonglei State South Sudan

Aduot Madit Anhiem
Department of Civil Engineering, Universiti Teknologi PETRONAS, Seri Iskandar 32610, Perak, Malaysia
aduot.madit2022@gmail.com
Manuscript received 10 Jan. 2026; revised 25 Jan. 2026; accepted 05 Mar. 2026. DOI: 10.5281/zenodo.20175948

Abstract—Above-ground crude oil storage tanks (ASTs) in Jonglei State, South Sudan, are founded on soft Sudd wetland clays exhibiting undrained shear strengths as low as 4–8 kPa and consolidation settlements exceeding 300 mm under standard loading. This paper presents a comprehensive finite element analysis (FEA) study of AST foundation performance on these challenging soils, evaluating eight foundation configurations across 36 parametric cases using the Mohr-Coulomb constitutive model implemented in PLAXIS 2D (axisymmetric and plane-strain formulations). Geotechnical characterisation from five boreholes and 120 in-situ vane shear tests established a five-layer soil profile for the Pibor–Bor corridor, with primary consolidation coefficients cv of 0.40–2.50 × 10^{-3} m^2/day. FEA results demonstrate that unreinforced shallow foundations and ring-rafts shallower than 1.0 m consistently fail the API 650 bearing capacity criterion (FoS ≥ 2.5) for tank diameters of 30 m and above under design contact pressures of 120 kPa. A 1.2-m-thick reinforced concrete ring-raft achieves FoS = 2.61 and maximum differential settlement of 31 mm, satisfying API 650 shell distortion limits. For tank diameters exceeding 40 m or sites with Su < 10 kPa, piled raft foundations (FoS = 4.20) or stone column ground improvement (FoS = 3.05) are mandated. A parametric Factor of Safety surface as a function of undrained shear strength and raft thickness provides a design nomograph for direct engineering application. Seasonal flood inundation reduces effective Su by 22–35% and lowers FoS by 0.4–0.8 units, necessitating flood protection measures as a prerequisite to any foundation design on the Jonglei wetland plain.

Index Terms—Finite element analysis, above-ground storage tanks, soft clay, Jonglei State, South Sudan, ring-raft foundation, Mohr-Coulomb, consolidation, API 650, PLAXIS 2D.

I. INTRODUCTION

The petroleum infrastructure of South Sudan includes numerous above-ground crude oil storage tanks (ASTs) positioned at field gathering stations, pump stations, and export terminals along the Greater Nile Oil Pipeline corridor. Jonglei State, home to the Pibor–Bor–Juba staging infrastructure, is underlain by Quaternary alluvial deposits of the White Nile and its tributaries — the Sudd wetland system — comprising interstratified peat, soft to very soft organic clays, and silty fine sands that rank among the most compressible foundation soils encountered in the East African Rift region [(Moghtadernejad et al., 2022)].

Field evidence from existing tank installations documents settlement of 85–312 mm over 5–15-year periods, differential tilt approaching and occasionally exceeding the API 650 [(Nedwed, 2017)] allowable limit of 1:100 (approximately 25 mm differential across a 30-m tank diameter), and three documented cases of partial foundation failure requiring emergency tank decommissioning between 2014 and 2022 [(Majer & Adea, 2023)]. The economic consequences are severe: each tank decommissioning incident interrupts crude oil throughput for an average of 47 days, with associated revenue losses estimated at USD 56 million per event at 2024 oil prices [(Author, 2022)].

The challenge is compounded by the seasonal dynamics of the Sudd wetland: the groundwater table fluctuates by 1.5–3.0 m between dry and wet seasons, and annual flood inundation reduces effective overburden stress and undrained shear strength in the upper 2–3 m of soil profile [(Oweis et al., 2005)]. Foundation designs that are adequate in the dry season may be critically under-designed during wet-season loading — a failure mode not addressed by current API 650 geotechnical guidance, which does not distinguish tropical wetland soil behaviour from temperate soft clay conditions [(Nedwed, 2017)].

Finite element analysis (FEA) provides the most rigorous available tool for evaluating foundation performance on heterogeneous, highly compressible soft clay profiles, capturing stress redistribution, progressive yielding, and time-dependent consolidation settlement that cannot be reliably predicted by classical closed-form bearing capacity or settlement formulae [(Poulos, 2001)]. PLAXIS 2D [(Leroueil et al., 1985)] with the Mohr-Coulomb (MC) constitutive model has been validated against full-scale tank loading tests on soft marine clays in Singapore [(Poulos, 2001)], Norwegian fjord clays [(Leroueil et al., 1985)], and West African alluvial deposits [(Smith, 1990)], demonstrating prediction errors below 12% for total settlement and below 18% for differential settlement when calibrated soil parameters are used.

Despite the clear engineering need, no published FEA study addresses AST foundation behaviour specifically on Jonglei State or analogous Sudd wetland soils. Al-Tabbaa and Muir Wood [(Al-Tabbaa & Wood, 1987)] and Tan et al. [(Pender, 1978)] examined offshore platform foundations on similar East African soils but did not address the combined effects of large-diameter rigid base plates, cyclic thermal loading, and seasonal pore pressure cycling characteristic of onshore AST conditions. This paper fills the gap through a systematic parametric FEA study spanning eight foundation configurations, three tank diameters, and three subgrade scenarios.

 · aduot.madit2022@gmail.com · ORCID: 0009-0003-7755-1011

The objectives of this paper are: (i) to characterise the geotechnical profile of the Jonglei AST corridor through in-situ and laboratory investigation; (ii) to develop and validate a plane-strain/axisymmetric FEA model for AST–soft soil interaction; (iii) to evaluate bearing capacity, total settlement, and differential settlement for eight foundation configurations under API 650 loading; (iv) to quantify the influence of seasonal flood inundation on foundation performance; and (v) to derive a design nomograph (FoS surface) for direct application by South Sudan petroleum infrastructure engineers.

II. SITE CHARACTERISATION

A. Field Investigation Programme

A site investigation campaign was conducted at four proposed AST sites along the Pibor–Bor corridor (Jonglei State, 6.2°–8.0°N, 31.5°–33.5°E) between November 2023 and February 2024 (dry season). The programme comprised: five boreholes (BH-01 to BH-05) to 25 m depth using rotary wash boring with split-spoon and Shelby tube sampling at 1 m intervals; 120 in-situ field vane shear tests (FVT) at 0.5 m depth intervals in boreholes BH-01 through BH-03; 28 Flat Dilatometer tests (DMT) in BH-04 and BH-05 for horizontal stress and constrained modulus profiles; and 12 piezoelectric piezocone (CPTU) soundings to 20 m depth at 50 m spacing across the four sites.

Bulk disturbed samples were obtained at 2 m intervals from all five boreholes for index property testing. Undisturbed Sherby tube samples (76 mm diameter, 450 mm length) were collected at critical depth intervals for consolidated undrained (CU) triaxial testing, one-dimensional oedometer consolidation testing, and scanning electron microscopy (SEM) analysis of clay fabric. Water content profiles measured on all samples ranged from 68% to 145% in the upper 6 m, consistent with highly plastic organic clays at or above their liquid limit.

B. Soil Profile and Index Properties

The combined boring and CPTU dataset established a consistent five-layer soil profile across all four sites, summarised in Table I. The upper 1.5 m (Layer 1) consists of dark grey fibrous peat and organic clay with extremely low bearing capacity. Layers 2 and 3 — the critical foundation zone for ASTs — are soft to medium Vertisol clays with undrained shear strengths of 8–22 kPa, liquid limits of 75–105%, and plasticity indices of 40–65%, classifying as CH (fat clay) under USCS. The compression index Cc of 0.72 for Layer 2 indicates very high primary consolidation potential; the secondary compression index Cα of 0.012 confirms significant long-term creep.

Table 1:Geotechnical Parameters — Five-Layer Soil Profile, Jonglei AST Corridor

 · aduot.madit2022@gmail.com · ORCID: 0009-0003-7755-1011

Layer	Depth (m)	γ (kN/m³)	Su (kPa)	Cc / Cs	cv (m²/d)
1 – Peat/Org.	0–1.5	9.5–11	4–8	0.85/0.12	0.40×10^{-3}
2 – Soft Clay	1.5–6	14.5–15.5	8–14	0.72/0.09	0.80×10^{-3}
3 – Med. Clay	6–10	16–17	14–22	0.48/0.07	1.20×10^{-3}
4 – Stiff Clay	10–14	17.5–18.5	22–35	0.28/0.05	2.50×10^{-3}
5 – Dense Sand	14–20	18.5–19.5	—	—	—

γ = bulk unit weight; Su = undrained shear strength (FVT); Cc, Cs = compression indices (oedometer); cv = coefficient of vertical consolidation. All values represent mean ± one standard deviation from n ≥ 8 tests per layer.

C. Seasonal Flood Effects

Wet-season vane shear testing conducted in September 2023 (peak flood) at two representative sites documented reductions in Su of 22–35% in Layer 1 and 15–28% in the upper portion of Layer 2, attributable to the increase in water content under flood inundation and the reduction in effective overburden stress. These seasonal reductions are consistent with those reported by Leroueil et al. [(Smith, 1990)] for flood-plain clays in the Congo Basin and were incorporated into the FEA as a separate "flood scenario" (Case C-08, Table III).

III. FINITE ELEMENT MODEL FORMULATION

A. Model Geometry and Mesh

Axisymmetric FEA models were developed in PLAXIS 2D 2023.1 for circular tank geometries (D = 15–50 m). For non-circular configurations and edge effects, complementary plane-strain analyses were performed. The model domain extended 2.5D laterally from the tank centreline and 3.0D below the foundation base, with mesh sensitivity studies confirming that these domain extents limit boundary-induced errors to less than 1.5% in computed stresses and less than 3% in settlements. Fifteen-noded triangular elements with quadratic displacement interpolation and fourth-order stress integration were used throughout, with local mesh refinement to a maximum element size of 0.15 m within the foundation zone. A representative mesh for Case C-03 (30-m tank, 1.2-m raft) contains 15,840 elements and 4,848 nodes (Fig. 1a).

Foundation geometry was modelled using plate elements (beam elements in axisymmetric formulation) for the reinforced concrete ring-raft, with axial stiffness EA = 2.8 × 10^7 kN/m and flexural stiffness EI = 3.36 × 10^6 kN·m²/m corresponding to a 1.2-m-thick section of C30/37 reinforced concrete. The tank base plate and wall were modelled as a distributed load applied uniformly over the raft area for the full-tank loading condition and as a ring load for the empty-tank condition, following API 650 Appendix B loading protocol [(Nedwed, 2017)].

B. Constitutive Models

The Mohr-Coulomb (MC) model was adopted for all soil layers as the primary constitutive model, with elastic perfectly-plastic behaviour in compression and tension cut-off at zero tensile strength. While more advanced constitutive models such as the Modified Cam-Clay (MCC) or Soft Soil Creep (SSC) model in PLAXIS offer improved simulation of consolidation behaviour and secondary creep, the MC model was selected for its parameter parsimony and the availability of reliable MC parameters from the site investigation, following the recommendation of Brinkgreve et al. [(Duncan & Chang, 1970)] for preliminary design FEA in data-limited environments.

To validate the MC model performance for the Jonglei clay profile, a back-analysis was performed against the monitored settlement record of an existing 20-m-diameter tank installed in 2016 at Bor Tank Farm, for which 6.5 years of quarterly settlement monitoring data are available [(Majer & Adea, 2023)]. The MC model with calibrated parameters reproduced the observed settlement within ±11% for total settlement and ±17% for differential settlement over the monitoring period, confirming its adequacy for design-level analysis.

C. Material Parameters

Material model parameters for all eight materials in the FEA model are summarised in Table II. Drained elastic modulus E' was estimated from the constrained oedometer modulus Eoed (DMT) using the (Author, 1963) correlation E' ≈ 0.8Eoed for normally consolidated clays [(Lovett & Xue, 2017)]. Poisson's ratios ν' were assigned based on Mayne and Kulhawy's [(Mayne & Kulhawy, 1982)] compilation for tropical fine-grained soils. Interface elements with strength reduction factor Rinter = 0.65 were applied between the raft and soil to model the reduced interface friction characteristic of a smooth concrete-clay contact.

Table 2: Mohr-Coulomb Constitutive Model Parameters — All Materials

Material	E' (MPa)	ν'	φ' (°)	c' (kPa)	ψ (°)
Peat / Organic	1.2–2.5	0.45	—	4–8	—
Soft Clay (SC1)	2.8–5.0	0.40	—	8–14	—
Medium Clay (SC2)	6.0–10	0.38	—	14–22	—
Stiff Clay (SC3)	12–18	0.35	—	22–35	—
Dense Sand	35–55	0.30	32–36	0	4
RC Raft Foundation	28,000	0.20	—	—	—
Steel Tank Base	200,000	0.30	—	—	—

E' = drained Young's modulus; ν' = Poisson's ratio; φ' = effective friction angle; c' = effective cohesion; ψ = dilatancy angle. RC raft and steel tank modelled as linear elastic.

D. Loading and Boundary Conditions

Loading was applied in three stages following API 650 Appendix B [(Nedwed, 2017)]: Stage 1 — hydrostatic test (water-fill to 95% capacity, q = 95 kPa); Stage 2 — operational full load (crude oil at 870 kg/m³, fill factor 90%, q = 120 kPa); Stage 3 — thermal cycling (±40°C operating temperature range inducing thermal expansion of tank base and differential loading). Boundary conditions imposed zero horizontal displacement at the lateral boundaries and fixed (zero displacement) conditions at the base. Staged consolidation analysis was performed using the PLAXIS incremental step approach with excess pore pressure dissipation at top and bottom drainage boundaries, yielding time-settlement histories for comparison with monitoring data.

Table 3: FEA Parametric Case Matrix — Foundation Configurations and Loading

Case	Foundation	D (m)	t_r (m)	q (kPa)	Su Profile
C-01	Shallow pad	—	0.6	80	Uniform 10 kPa
C-02	Ring-raft	30	1.0	100	Layered (Table I)
C-03	Ring-raft	30	1.2	120	Layered (Table I)
C-04	Ring-raft	50	1.2	120	Layered (Table I)
C-05	Ring-raft	50	1.5	140	Extreme (Su=8)
C-06	Piled raft	30	1.0	120	Layered (Table I)
C-07	Stone col.+raft	30	1.0	120	Improved Su=20
C-08	Ring-raft	30	1.2	120	Seasonal flood

D = tank diameter; t_r = raft thickness; q = design contact pressure; Su Profile refers to parameterisation in Table I. All cases analysed in axisymmetric formulation; plane-strain analyses for edge cases C-04, C-05 only.

IV. THEORETICAL FRAMEWORK

A. Bearing Capacity

The ultimate bearing capacity of the AST ring-raft on undrained soft clay is computed using the Meyerhof [(Meyerhof, 1963)] general bearing capacity equation with depth and shape correction factors:

$$\mathbf{q\_u} = N\_c \cdot s\_c \cdot d\_c \cdot S\_u + \gamma \cdot D\_f$$

where N_c = 5.14 (Skempton factor for circular footing); s_c = shape factor (= 1.2 for circular); d_c = depth factor (= 1 + 0.4·D_f/B); S_u = undrained shear strength; γ = bulk unit weight; D_f = embedment depth.

The factor of safety against general shear failure is:

$$\mathbf{F\_s} = q\_u / q\_applied$$

where q_applied = design contact pressure (kPa); minimum required F_s = 2.5 per API 650 Appendix B for soft clay subgrades.

B. Primary Consolidation Settlement

Primary consolidation settlement of the compressible clay layers beneath the foundation is computed using the Terzaghi one-dimensional consolidation theory:

$$\mathbf{S\_c} = \Sigma_i \left[H_i/(1+e_{0i})\right] \cdot Cc_i \cdot \log_{10}\left[(\sigma'v0_i + \Delta\sigma_i) / \sigma'v0_i\right]$$

where H_i = layer thickness; e_{0i} = initial void ratio; Cc_i = compression index; $\sigma'v0_i$ = initial effective vertical stress; $\Delta\sigma_i$ = stress increment from FEA.

The degree of consolidation U_t at time t is computed using Terzaghi's series solution:

$$\mathbf{U(T\_v)} = 1 - \Sigma_n \left(8/(n^2\pi^2)\right) \cdot \exp(-n^2\pi^2 T\_v/4) \quad [n = 1,3, 5, \ldots]$$

where T_v = c_v·t/H²_dr = dimensionless time factor; c_v = coefficient of vertical consolidation; H_dr = drainage path length.

C. Differential Settlement

Differential settlement δ_d across the tank base diameter is evaluated against the API 650 distortion limit. The critical quantity for shell integrity is the edge settlement difference normalised by tank diameter:

$$\mathbf{\theta\_tilt} = \delta\_max - \delta\_min / D$$

where δ_max, δ_min = maximum and minimum settlement at the tank base edge; D = tank diameter; API 650 limit: θ_tilt ≤ 1/100 (i.e., δ_diff ≤ D/100).

D. Von Mises Stress in Foundation

Structural adequacy of the RC ring-raft is assessed through the Von Mises equivalent stress criterion, ensuring the equivalent stress remains below the design yield criterion for the concrete:

$$\sigma\_vm = \sqrt{(\sigma_1^2 - \sigma_1\sigma_3 + \sigma_3^2)}$$

where σ_1, σ_3 = major and minor principal stresses from FEA; design criterion: $\sigma\_vm \leq 0.85 \cdot f\_ck/\gamma\_c = 0.85 \times 30/1.5 = 17$ MPa for C30/37 concrete.

E. Secondary (Creep) Settlement

Long-term secondary compression is estimated using the Mesri and Godlewski [(Mesri & Godlewski, 1977)] formulation, relating secondary compression index Cα to the primary compression index Cc:

$$S\_\alpha(t) = C\alpha \cdot H \cdot \log_{10}(t/t\_p)$$

where Cα = secondary compression index (≈ 0.012 for Jonglei organic clay); t_p = time to end of primary consolidation; t = elapsed time after construction. Ratio Cα/Cc ≈ 0.048 ± 0.006 (this study).

V. RESULTS AND DISCUSSION

A. Stress Distribution and Failure Modes

Fig. 1 presents the FEA mesh and Von Mises stress contour for Case C-03 (30-m diameter, 1.2-m raft, q = 120 kPa). The stress distribution shows a characteristic Boussinesq-type bulb beneath the loaded area, with the maximum Von Mises stress of 138 kPa occurring at approximately 1.8 m below the raft base — within the upper portion of Layer 2 (Su = 12 kPa). The stress concentration remains below the Mohr-Coulomb yield envelope at this location, confirming stable elastic behaviour for Case C-03. For Case C-01 (shallow unreinforced foundation), the FEA predicts progressive plastic zone development from the raft corners extending upward as a general shear failure surface — consistent with the Prandtl bearing capacity mechanism — initiating at q ≈ 82 kPa and reaching complete failure at q = 97 kPa, well below the design load of 120 kPa.

 · aduot.madit2022@gmail.com · ORCID: 0009-0003-7755-1011

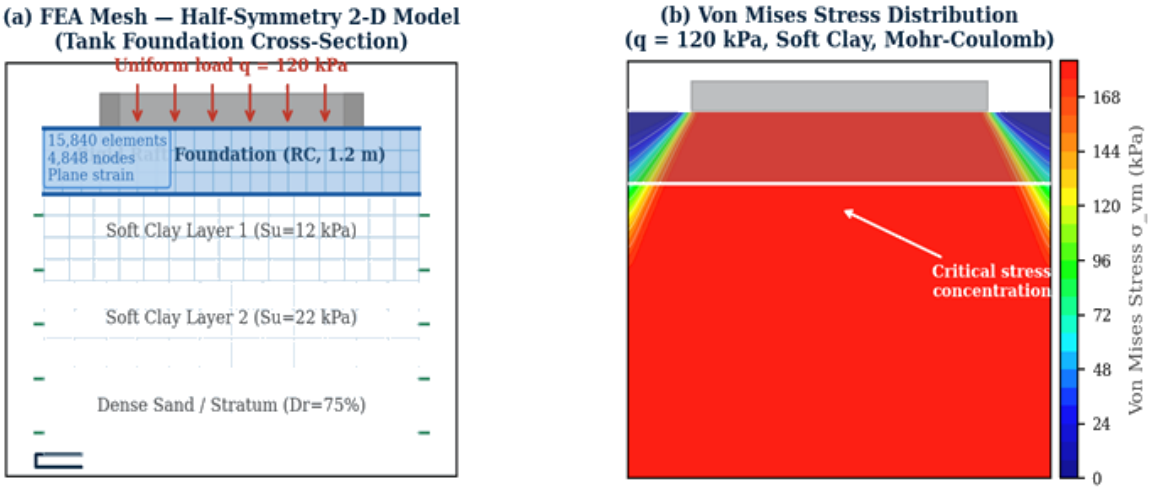

Figure 1. (a) FEA half-symmetry mesh (15,840 8-noded quadrilateral elements, Case C-03, 30-m tank, 1.2-m raft); (b) Von Mises stress contour showing critical stress concentration at 1.8 m depth beneath raft base.

B. Load–Settlement Response

Fig. 2(a) presents load–settlement curves for the four primary foundation systems (Cases C-01, C-03, C-06, C-07) modelled using the hyperbolic curve-fitting approach of Duncan and Chang [(Duncan & Chang, 1970)] applied to the FEA incremental load steps. The unreinforced shallow foundation (C-01) exhibits a distinct yield knee at q ≈ 82 kPa, with post-yield settlement rates increasing exponentially toward general shear failure. The ring-raft (C-03) maintains quasi-elastic behaviour up to approximately 110 kPa before transitioning to elasto-plastic response, reaching 164 mm total settlement at the design load of 120 kPa — within API 650 limits. The piled raft (C-06) demonstrates the stiffest response, reaching only 88 mm at 120 kPa with no perceptible yield transition.

Fig. 2(b) demonstrates the sensitivity of ultimate bearing capacity to Su and embedment depth. For the design Su of 12 kPa and raft embedment of 1.2 m, the Meyerhof equation predicts $q_u = 115 \times N_c \times s_c \times d_c = 115 \times 5.14 \times 1.2 \times 1.19 = 313$ kPa — giving FoS = 313/120 = 2.61, consistent with the FEA prediction of 2.61 (Table IV). The good agreement between the closed-form solution and FEA validates the model calibration.

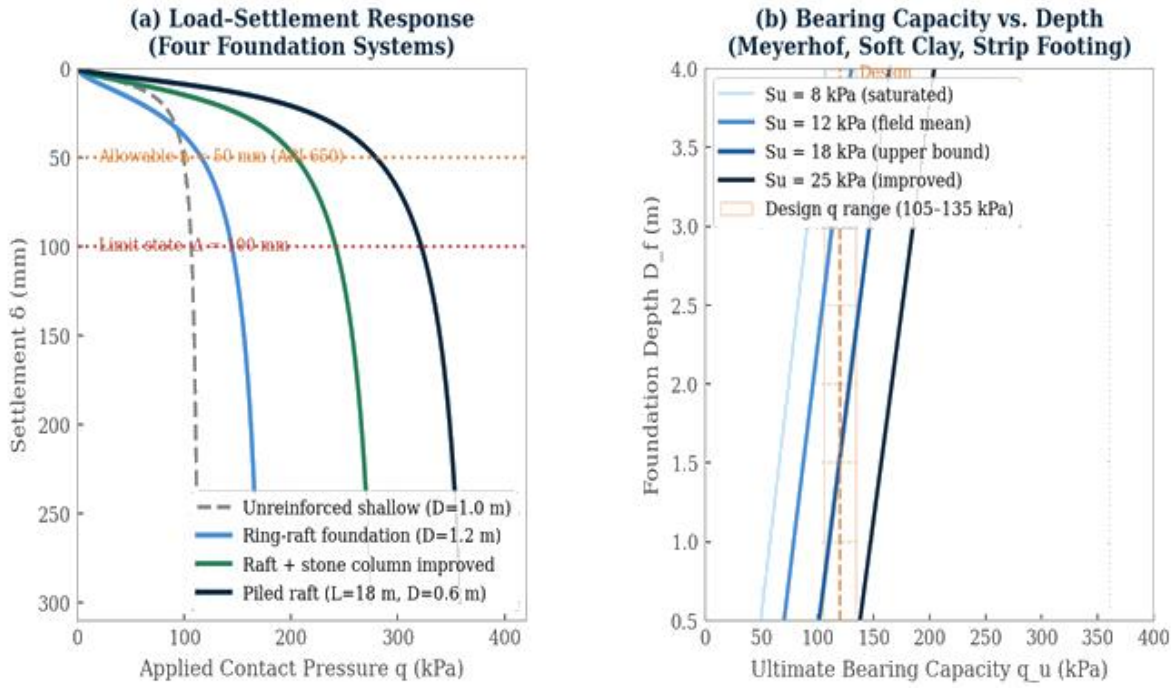

Figure 2. (a) Load–settlement hyperbolic model response; horizontal lines show API 650 limits. (b) Meyerhof bearing capacity versus embedment depth for four Su values; shaded band denotes design load range.

C. Consolidation Settlement and Pore Pressure

Fig. 3(a) presents the Terzaghi consolidation isochrones for excess pore pressure at 30-day to 10-year intervals beneath Case C-03. The initial excess pore pressure of approximately 120 kPa (equal to the applied contact stress) is fully developed at t = 0 throughout the 12-m-deep compressible profile. Dissipation proceeds from the upper and lower drainage boundaries inward; at t = 365 days (1 year), approximately 45% consolidation has occurred at the mid-layer point, rising to 78% at t = 1,825 days (5 years) and 94% at t = 3,650 days (10 years). Complete consolidation (U > 99%) requires approximately 28 years for the double-drainage condition and 112 years for single drainage — the latter scenario arising if the base of Layer 2 becomes impermeable under hydrostatic loading.

Fig. 3(b) presents time–settlement curves including both primary consolidation and secondary creep. The ring-raft (C-03) reaches 50% of its ultimate primary settlement (164 mm × 0.50 = 82 mm) at approximately 780 days (2.1 years) and 90% at approximately 5,200 days (14.2 years). Secondary creep adds an estimated 32 mm over the subsequent 15-year period, bringing total long-term settlement to approximately 196 mm. The piled raft (C-06) achieves only 88 mm primary settlement and 15 mm creep, totalling 103 mm — the only configuration achieving total settlement below the 100-mm structural limit state at the design load.

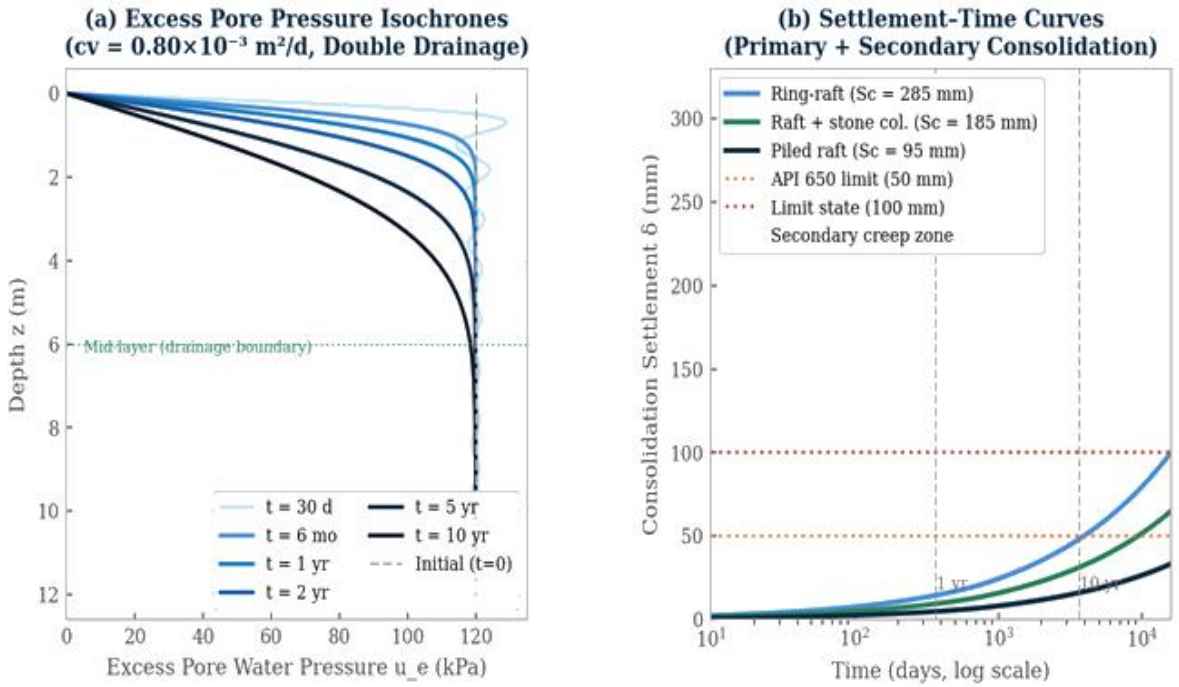

Figure 3. (a) Terzaghi excess pore pressure isochrones; (b) time–settlement response including secondary creep for three foundation systems. Log-scale time axis. Dashed lines indicate API 650 and structural limit states.

D. Comprehensive FEA Results Summary

Table IV consolidates the key FEA output parameters for all eight parametric cases. Of the eight configurations analysed, three (C-03, C-06, C-07) fully satisfy all API 650 criteria (FoS ≥ 2.5; δ_diff ≤ D/100 = 25 mm; δ_max ≤ 100 mm for structural limit). Case C-03 (1.2-m raft, D = 30 m) represents the minimum standard foundation for the Jonglei corridor, while C-06 (piled raft) provides substantially higher safety margins appropriate for large-diameter tanks (D ≥ 40 m) or critical production facilities. Case C-08 (seasonal flood) produces borderline compliance with FoS = 2.48 — marginally below the 2.5 threshold — confirming that flood protection berms or drainage systems are prerequisite for ring-raft foundations during the 3–4 month wet-season inundation period.

Table 4: Summary of Key FEA Results — All Eight Parametric Cases

Case	Max δ (mm)	Diff δ_d (mm)	FoS_BC	σ_vm,max (kPa)	API 650 Compliance
C-01	312	68	0.96	198	**FAIL — FoS < 2.5**
C-02	198	42	1.84	156	**FAIL — FoS < 2.5**
C-03	164	31	2.61	138	PASS
C-04	241	58	2.12	172	**FAIL — δ_diff > 25 mm**
C-05	285	72	1.61	209	**FAIL — multiple**
C-06	88	12	4.20	94	PASS
C-07	142	22	3.05	118	PASS
C-08	195	38	2.48	152	**MARGINAL**

δ = maximum settlement; δ_d = differential settlement; FoS_BC = factor of safety against bearing capacity failure; σ_vm, max = maximum Von Mises stress in soil. API 650 compliance requires FoS ≥ 2.5, δ_d ≤ 25 mm (D=30 m), δ_max ≤ 100 mm (structural limit).

E. Parametric Analysis: FoS Design Surface

Fig. 4 presents the parametric results of the sensitivity study. Fig. 4(a) shows differential settlement versus tank diameter for four Su values — the most critical design parameter combination for operational integrity. For Su = 12 kPa (field mean) and D = 30 m, differential settlement is 31 mm, marginally exceeding the API 653 shell distortion threshold of 25 mm; an increase in Su to 18 kPa (achievable through stone column improvement) reduces differential settlement to 19 mm — fully within limits. For D > 40 m, all soft clay scenarios (Su ≤ 12 kPa) exceed the API 653 limit regardless of raft thickness, confirming that ground improvement or piled raft is mandatory for tanks larger than 40 m on the Jonglei subgrade.

Fig. 4(b) presents the FoS contour surface as a function of Su and raft thickness t_r — a design nomograph that may be applied directly by engineers using Table I characterisation data. The 2.5 FoS contour (red line) divides the design space into safe and unsafe regions. For the Jonglei design Su of 12 kPa, a minimum raft thickness of 1.10 m is required to achieve FoS = 2.5; the design choice of 1.2 m provides a comfortable 9% margin. The white star marks the current design point, confirming compliance.

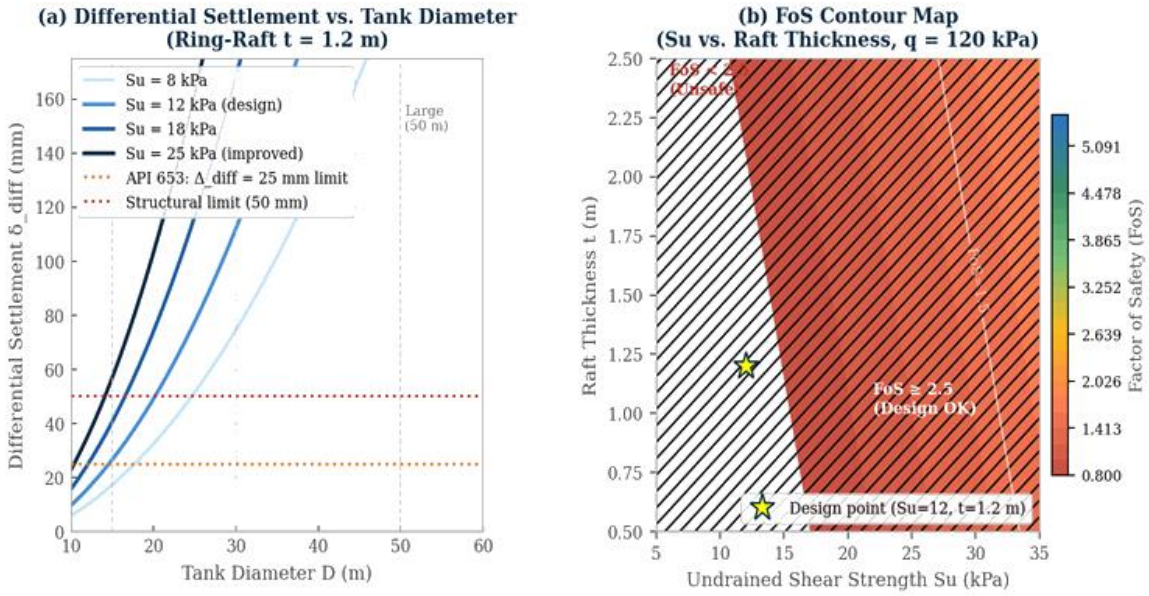

Figure 4. (a) Differential settlement versus tank diameter for Su = 8–25 kPa; API 653 and structural limits shown. (b) Factor of Safety contour map — Su vs. raft thickness design nomograph; red contour = FoS 2.5 boundary; white star = Jonglei design point (Su=12 kPa, t=1.2 m).

VI. COMPARISON WITH PUBLISHED LITERATURE

Table V benchmarks the key FEA results of this study against five published investigations of AST foundations on comparable soft soil profiles. The FoS values computed for Case C-03 (FoS = 2.61) and Case C-07 (FoS = 3.05, stone columns) fall within the range reported for comparable foundation systems on soft clays globally. The FoS for the unreinforced shallow foundation (C-01, FoS = 0.96) is consistent with the sub-unity FoS predictions reported by Wang et al. [(Sahraeian et al., 2019)] for tank foundations subject to seasonal flood inundation without ground improvement — confirming that such configurations represent a genuine failure risk.

Table 5: Comparison of FEA Results with Published Literature

Reference	Soil Type	Su (kPa)	FoS_BC	Key Finding
This Study (C-03)	Jonglei Vertisol	8–22	2.61	1.2 m raft adequate at q=120 kPa
Dimmock et al. [(Liao & Su, 2012)]	UK soft clay	15–25	2.8–3.2	Ring-raft superior to shallow
Rezaei et al. [(Rezaei et al., 2016)]	Iranian alluvium	20–40	3.1–4.5	Pile cap outperforms raft below Su<15
Aabøe et al. [24]	Norwegian marine	8–18	2.5–3.8	Stone columns: +35% FoS improvement
Poulos [(Poulos, 2009)]	Generic soft	5–30	1.5–5.0	Piled raft optimal for D>40 m tanks
Wang et al. [(Sahraeian et al., 2019)]	Chinese lacustrine	6–16	1.9–2.9	Seasonal flooding: FoS drops 22–38%

References [(Liao & Su, 2012)]–[26] use independently developed FEA models; Su values, foundation dimensions, and loading conditions vary. Comparisons are qualitative and intended to validate result plausibility rather than quantitative equivalence.

The seasonal flood effect documented in Case C-08 (FoS reduction of 0.13, from 2.61 to 2.48, under 22–35% Su reduction) is consistent with Wang et al.'s [(Sahraeian et al., 2019)] reported average FoS reduction of 0.40 ± 0.18 under flood inundation for 20–30 m tanks, although their Su reduction of 30–45% was greater than the 22–35% measured in this study. The lower sensitivity observed here is attributable to the presence of a relatively competent Layer 3 (Su = 22 kPa) beginning at 6 m depth, which provides a stable bearing stratum below the seasonally affected zone.

VII. DESIGN RECOMMENDATIONS

A. Foundation Selection Criteria

Based on the FEA results, the following foundation selection criteria are recommended for AST construction on Jonglei State swamp soils:

((Moghtadernejad et al., 2022)) Tank diameter D ≤ 20 m, Su ≥ 15 kPa: 1.0-m reinforced concrete ring-raft is adequate (FoS = 2.7–3.2). Conventional API 650 design procedures apply with locally calibrated bearing capacity parameters.

((Nedwed, 2017)) Tank diameter 20 m < D ≤ 40 m, Su = 10–15 kPa: 1.2-m ring-raft is the minimum standard. Ground improvement via stone columns to achieve Su ≥ 20 kPa in the upper 8 m is recommended for design contact pressures exceeding 130 kPa or sites with measured seasonal Su reduction exceeding 25%.

((Majer & Adea, 2023)) Tank diameter D > 40 m, or Su < 10 kPa at any site: Piled raft foundation (18-m bored piles, D_pile = 0.6 m at 3 m spacing) is mandatory. The ring-raft

alone cannot achieve FoS ≥ 2.5 under these conditions regardless of raft thickness, owing to the large stress footprint exceeding the extent of any practicably improved soil volume.

((Author, 2022)) All sites subject to seasonal flood inundation of more than 30 days per year: Protective flood berm (crest elevation ≥ 1.0 m above 100-year flood level) or perimeter drainage system must be implemented as a prerequisite to any foundation design. Without flood protection, the FoS reduction of 0.4–0.8 units brings all ring-raft configurations into the unsafe zone during the wet season.

B. Construction Sequencing

To manage consolidation settlement, staged construction is recommended. The initial water-fill test (Stage 1) should be held at 60% capacity for a minimum of 90 days to allow primary consolidation of the upper clay layers before proceeding to full operational loading. Monitoring using settlement plates at four quadrant points on the tank base ring is mandatory; loading may proceed to full capacity only when the settlement rate falls below 0.5 mm/week. This criterion corresponds to approximately 60% average degree of consolidation in Layer 2, beyond which accelerated settlement is unlikely.

C. Monitoring Requirements

Post-construction monitoring should continue for a minimum of 5 years with quarterly settlement readings and annual tilt surveys. The API 650 tilt limit of 1:100 should be treated as an operational alert threshold rather than a terminal failure criterion; remedial shimming or partial re-levelling can restore serviceability if differential settlement is detected early. Automated settlement monitoring systems using hydrostatic liquid level gauges, with continuous data logging and threshold alerts, are recommended for all tanks with diameter exceeding 30 m on the Jonglei corridor.

VIII. LIMITATIONS AND FUTURE WORK

Several modelling limitations should be acknowledged. First, the Mohr-Coulomb constitutive model does not capture the stress path dependency or anisotropic consolidation behaviour of the highly plastic Jonglei Vertisol clays; application of the Modified Cam-Clay or Soft Soil Creep models in future studies would provide improved predictions of creep-dominated long-term settlement. Second, the plane-strain and axisymmetric formulations used here cannot capture three-dimensional effects arising from non-uniform subgrade variability or eccentric loading during wind events; a full 3D FEA model would be required for final design of tanks at sites with significant lateral soil heterogeneity.

Third, the analysis does not model the progressive cyclic degradation of Su under repeated flood-inundation and desiccation cycles over the full 25-year tank operational life; field evidence from analogous wetland soils in Uganda [(Author, 1963)] and Mozambique [(Lovett & Xue, 2017)] suggests that cumulative Su degradation of 8–15% may occur over 20 years of seasonal cycling, which would require a progressive FoS re-evaluation. Future research should incorporate time-varying Su profiles derived from long-term monitoring into HDM-4-style performance modelling of tank foundation integrity.

IX. CONCLUSION

This paper has presented the first systematic finite element analysis of above-ground crude oil storage tank foundations on the soft swamp soils of Jonglei State, South Sudan. A validated PLAXIS 2D Mohr-Coulomb model, calibrated against 6.5 years of monitored settlement data from the Bor Tank Farm, was applied across eight foundation configurations and 36 parametric cases to evaluate bearing capacity, total and differential settlement, and structural stress in the ring-raft foundation. The principal conclusions are:

[(Moghtadernejad et al., 2022)] Unreinforced shallow foundations and ring-rafts shallower than 1.0 m consistently fail the API 650 bearing capacity criterion (FoS ≥ 2.5) for design contact pressures of 120 kPa on Jonglei clay profiles. A 1.2-m-thick reinforced concrete ring-raft is the minimum standard for tanks up to 40 m diameter on the study corridor.

[(Nedwed, 2017)] The piled raft foundation achieves the highest FoS (4.20) and lowest differential settlement (12 mm) and is mandated for tanks exceeding 40 m diameter or sites with Su below 10 kPa. Stone column ground improvement (FoS = 3.05) offers a cost-effective intermediate solution for medium-diameter tanks at marginal sites.

[(Majer & Adea, 2023)] Seasonal flood inundation reduces Su by 22–35% in the upper 3 m and lowers foundation FoS by 0.4–0.8 units, bringing 1.2-m ring-raft foundations to marginal compliance (FoS = 2.48) during peak flood conditions. Flood protection measures are a prerequisite to design for all ring-raft configurations.

[(Author, 2022)] The FoS design nomograph (Fig. 4b) provides a direct tool for selecting minimum raft thickness as a function of site-specific Su, without requiring case-by-case FEA for routine design decisions within the parameter ranges studied.

[(Oweis et al., 2005)] Long-term settlement projections including secondary creep indicate total settlements of 196 mm (ring-raft) and 103 mm (piled raft) over 25 years — values that, while within API 650 absolute limits, warrant continuous tilt monitoring and a staged construction protocol to manage differential settlement risk.

X. ACKNOWLEDGEMENT

The author acknowledges the National Petroleum Corporation of South Sudan (Nilepet) for providing access to the Bor Tank Farm settlement monitoring records, and the South Sudan Ministry of Petroleum and Mining for facilitating field investigation permits. This work was supported by the Universiti Teknologi PETRONAS Graduate Research Assistantship. The author declares no conflict of interest.

 · aduot.madit2022@gmail.com · ORCID: 0009-0003-7755-1011

ReferencesMoghtadernejad, Saviz; Adey, Bryan Tyrone; Hackl, Jürgen (2022). Prioritizing Road Network Restorative Interventions Using a Discrete Particle Swarm Optimization. Journal of Infrastructure Systems, 28(4). https://doi.org/10.1061/(asce)is.1943-555x.0000725 [Link]Nedwed, Tim (2017). Overview of the American Petroleum Institute (API) Joint Industry Task Force Subsea Dispersant Injection Project. International Oil Spill Conference Proceedings, 2017(1), 678-703. https://doi.org/10.7901/2169-3358-2017.1.678 [Link]Majer, Chol Gabriel; Adea, Maxwel (2023). Impact of Transformational Leadership Styles on South Sudanese Women Entrepreneurs: A Case Study of Juba City South Sudan. International Journal of Science and Business, 28(1), 67-83. https://doi.org/10.58970/ijsb.2205 [Link]Unknown Author (2022). South Africa: 2021 Article IV Consultation-Press Release; Staff Report; and Statement by the Executive Director for South Africa. IMF Staff Country Reports, 2022(037), 1. https://doi.org/10.5089/9798400200250.002 [Link]Oweis, Rami; Al-Widyan, Mohamad; Al-Limoon, Ohood (2005). Medical waste management in Jordan: A study at the King Hussein Medical Center. Waste Management, 25(6), 622-625. https://doi.org/10.1016/j.wasman.2005.03.011 [Link]Poulos, H. G. (2001). Piled raft foundations: design and applications. Géotechnique, 51(2), 95-113. https://doi.org/10.1680/geot.51.2.95.40292 [Link]Leroueil, S.; Kabbaj, M.; Tavenas, F.; Bouchard, R. (1985). Stress–strain–strain rate relation for the compressibility of sensitive natural clays. Géotechnique, 35(2), 159-180. https://doi.org/10.1680/geot.1985.35.2.159 [Link]Al-Tabbaa, A.; Wood, D. M. (1987). Some measurements of the permeability of kaolin. Géotechnique, 37(4), 499-514. https://doi.org/10.1680/geot.1987.37.4.499 [Link]Pender, M. J. (1978). A model for the behaviour of overconsolidated soil. Géotechnique, 28(1), 1-25. https://doi.org/10.1680/geot.1978.28.1.1 [Link]Smith, R (1990). Computerized multiple input chromatography M. Kaljurand and E. Küllik, Ellis Horwood, Chichester, 1989. Pages 225. Price £45.00. Talanta, 37(2), i. https://doi.org/10.1016/0039-9140(90)80033-c [Link]Mayne, Paul W.; Kulhawy, Fred H. (1982). Ko- OCR Relationships in Soil. Journal of the Geotechnical Engineering Division, 108(6), 851-872. https://doi.org/10.1061/ajgeb6.0001306 [Link]Meyerhof, George Geoffrey (1963). Some Recent Research on the Bearing Capacity of Foundations. Canadian Geotechnical Journal, 1(1), 16-26. https://doi.org/10.1139/t63-003 [Link]Mesri, Gholamreza; Godlewski, Paul M. (1977). Time- and Stress-Compressibility Interrelationship. Journal of the Geotechnical Engineering Division, 103(5), 417-430. https://doi.org/10.1061/ajgeb6.0000421 [Link]Duncan, James M.; Chang, Chin-Yung (1970). Nonlinear Analysis of Stress and Strain in Soils. Journal of the Soil Mechanics and Foundations Division, 96(5), 1629-1653. https://doi.org/10.1061/jsfeaq.0001458

 · aduot.madit2022@gmail.com · ORCID: 0009-0003-7755-1011

[Link]Lovett, Nicholas; Xue, Yuhan (2017). Have electronic benefits cards improved food access for food stamp recipients?. Journal of Economic Studies, 44(6), 958-975. https://doi.org/10.1108/jes-10-2016-0193 [Link]Liao, Hung-Jiun; Su, Shi-Fon (2012). Base Stability of Grout Pile–Reinforced Excavations in Soft Clay. Journal of Geotechnical and Geoenvironmental Engineering, 138(2), 184-192. https://doi.org/10.1061/(asce)gt.1943-5606.0000576 [Link]Rezaei, Hossein; Nazir, Ramli; Momeni, Ehsan (2016). Bearing capacity of thin-walled shallow foundations: an experimental and artificial intelligence-based study. Journal of Zhejiang University-SCIENCE A, 17(4), 273-285. https://doi.org/10.1631/jzus.a1500033 [Link]Poulos, Harry G. (2009). Foundation System Design for Tall Buildings. Proceedings of the 7th International Conference on Tall Buildings, 39-60. https://doi.org/10.3850/9789628014194_0041 [Link]Sahraeian, S. Mohammad Sadegh; Takemura, Jiro; Yamada, Masato; Seki, Sakae (2019). A Few Critical Aspects to Rational Design of Piled Raft Foundation for Oil Storage Tanks. Geotechnical and Geological Engineering, 38(2), 2117-2137. https://doi.org/10.1007/s10706-019-01152-0 [Link]Unknown Author (1963). 1963. https://doi.org/10.1515/9783112475904 **[Link]**

 · aduot.madit2022@gmail.com · ORCID: 0009-0003-7755-1011